Processing and Application of Ceramics 15 [3] (2021) 246–255
https://doi.org/10.2298/PAC2103246S

Study of composite TiN/Ag/Cu_2O/TiO_2 with improved photocatalytic performance

Xinwei Shi[1,*], Jing Li[1], Jingyu Zhu[1], Yifan Yang[1], Xiaoxia Wang[1], Bailin Zhu[2], Liujie Xu[3]

[1]*School of Physics and Microelectronics, Zhengzhou University, Zhengzhou 450001, China*
[2]*The State Key Laboratory of Refractories and Metallurgy, Wuhan University of Science and Technology, Wuhan 430081, China*
[3]*Henan Key Laboratory of High-temperature Structural and Functional Materials, Henan University of Science and Technology, Luoyang 471003, China*

Received 14 March 2021; Received in revised form 31 May 2021; Accepted 31 July 2021

Abstract

TiO_2 film has the advantage of good photochemical stability and it can be used for self-cleaning glasses. However, due to the wide band gap, the spectral response range of TiO_2 film is restricted to the ultraviolet region. In this work, based on the research of TiO_2 thin films, multilayer TiN/Ag/Cu_2O/TiO_2 films were designed and successfully prepared. The structure and properties of the obtained samples were characterized by X-ray diffraction, spectral ellipsometry (SE), atomic force microscopy (AFM) and UV-Vis-NIR spectrophotometer. The results show that p-n heterojunction will be formed between Cu_2O and TiO_2 in the multilayer film, thus reducing the band gap of TiO_2 film. Based on the analysis of the photocatalytic mechanism of the multilayer films, a conclusion may be drawn that the designed multilayer film is helpful to improve the photocatalytic efficiency of titanium dioxide and expand its utilization of sunlight.

Keywords: *TiO_2 thin film, photocatalytic efficiency, TiN/Ag/Cu_2O/TiO_2 multilayer films*

I. Introduction

Since the photocatalytic properties of titanium dioxide (TiO_2) were reported by Fujishima and Honda in 1972 [1,2], TiO_2 has attracted considerable attention [1] due to its excellent properties. They include excellent optical transmittance, high refractive index, high dielectric constant, chemical stability, better adhesion as well as photocatalytic performance, which give TiO_2 prospects for potential application in optical coating and self-cleaning [3]. Although it posses many superior properties, the industrial application of TiO_2 has made slow progress because of its polymorphic nature. As often described, TiO_2 has three kinds of crystal phases: anatase, rutile and brookite [2]. A given TiO_2 thin film with a particular phase composition generally has a specific optical, photocatalytic or photohydrophilic properties for a specific application. For example, anatase TiO_2 has good photoinduced superhydrophilicity and photocatalytic activity, which can be used for self-cleaning, anti-fogging, air purification [4], etc. However, due to its large band gap width (about 3.2 eV), anatase TiO_2 generates photo-generated carriers only when it is irradiated by ultraviolet light. It is well known that the ultraviolet light makes only less than 7% in sunlight, which greatly limits the application of TiO_2 in the field of photocatalysis. Therefore, how to reduce the band gap of anatase TiO_2 and improve its photocatalytic efficiency is of great significance.

In the present work, based on the research of sputtering time effect on the properties of TiO_2 thin film, multilayer film with TiN/Ag/Cu_2O/TiO_2 structure was designed. Studies have shown that bilayer TiN and TiO_2 film has catalytic and plasma effects, which make them suitable for self-cleaning and infrared detectors [5]. Silver is usually the preferred material for metal layers in multilayer thin films. On one hand, metals with low resistivity absorb less than 5% in the visible region and have high reflectivity in the infrared band. On the other hand, the recombination of Ag enables photogenerated electrons to transfer from the conduction band of Cu_2O

* Corresponding author: tel: +86 13837167882,
e-mail: *Shixw@zzu.edu.cn*

to Ag, which inhibits the recombination probability of electron-hole pairs. At the same time, Cu_2O band gap width decreases and impurity level is not introduced, which improves the photocatalytic activity of Cu_2O to a certain extent [6–8]. In Cu_2O/TiO_2 thin film system, the heterojunction formation of p-n type between Cu_2O with narrower bandwidth and TiO_2 with larger bandwidth makes the TiO_2 to produce carrier in the visible area. Hence, the photocatalytic activity of the system can be improved because the energy in the visible region accounts for about 50% of the solar radiation [9–14]. In a word, the multilayer film with $TiN/Ag/Cu_2O/TiO_2$ structure can effectively reduce the TiO_2 band gap width and extend the use of sunlight to the visible region, which improves its self-cleaning ability.

In this paper, magnetron sputtering method was used to obtain TiO_2 film and $TiN/Ag/Cu_2O/TiO_2$ multilayer film on glass substrate. The influence of sputtering time on the properties of the TiO_2 films was studied combined with the Essential MacLeod software. The optical properties and photocatalytic performance were examined in detail. It is proved that the proposed design of the multilayer film is an effective way to improve the photocatalytic performance of TiO_2 film.

II. Experimental

2.1. Preparation of TiO_2 films

TiO_2 thin films were prepared on glass substrates (25 mm × 25 mm × 1 mm) using a Ti target (99.999% in purity, 60 mm in diameter and 5 mm in height, Beijing Jingmai Zhongke Material Technology Co. Ltd) in DC-RF multifunctional magnetron sputtering apparatus (CS-300, Changshu Yuhua Vacuum Equipment Technology Co. Ltd). In order to obtain films with good adhesion, all substrates were washed in deionized water, anhydrous ethanol, acetone and anhydrous ethanol, respectively, in ultrasonic bath for 15 min before the experiment and stored in anhydrous ethanol for later use. When the vacuum chamber was evacuated to 8.0×10^{-4} Pa by molecular pump, high purity Ar (99.999%) was introduced into the reaction chamber and the target was bombarded for 10 min for pre-sputtering. Then high purity O_2 (99.999%) was introduced into the reaction chamber as reaction gas. The flow rates of Ar and O_2 gas were kept at 24 and 6 sccm, respectively. During the deposition process, the distance between the substrate and target was kept at 65 mm, the sputtering power was 220 W and the sputtering temperature was 473 K. The sputtering time was 10, 20 and 30 min and the obtained samples were labelled as S1, S2 and S3, respectively.

2.2. Preparation of $TiN/Ag/Cu_2O/TiO_2$ films

The structure of the $TiN/Ag/Cu_2O/TiO_2$ multilayer film was designed as shown in Fig. 1 and obtained in the same magnetron sputtering apparatus mentioned above.

TiN and TiO_2 layers were prepared by reactive magnetron sputtering (with Ti target 99.999% in purity),

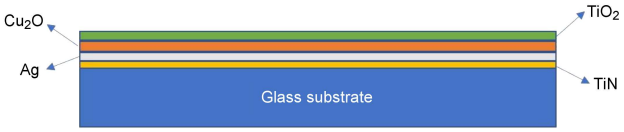

Figure 1. Schematic diagram of $TiN/Ag/Cu_2O/TiO_2$ multilayer film structure

Ag layer (with Ag target 99.999% in purity) was prepared by DC magnetron sputtering and Cu_2O layer (with Cu_2O target 99.999% in purity) was prepared by RF magnetron sputtering. All the targets were purchased from Beijing Jingmai Zhongke Material Technology Co. Ltd. During all layers deposition processes, the background vacuum reached 8×10^{-4} Pa. The sputtering times of TiN, Ag and Cu_2O layers were 100, 40 and 60 min, respectively. The sputtering time of TiO_2 film was 10, 20 and 30 min and the obtained multilayer films were labelled as CF1, CF2 and CF3, respectively. The parameters used for deposition of the multilayer films are listed in Table 1.

Table 1. Preparation process parameters of $TiN/Ag/Cu_2O/TiO_2$ multilayer film

Deposition process	TiN	Ag	Cu_2O	TiO_2
Power [W]	200	20	70	220
Pressure [Pa]	1.0	1.0	1.3	1.0
Flow rate of Ar [sccm]	15	20	46	24
Flow rate of N_2 [sccm]	2	0	0	0
Flow rate of O_2 [sccm]	0	0	0	6
Temperature [K]	473	298	473	473

2.3. Characterization of thin films

X-ray diffraction (XRD) data were obtained using an Empyrean CT tomography X-ray diffraction system at a scanning rate of 0.05 °/s under 45 kV and 40 mA Cu Kα radiation. Atomic force microscope (AFM, Model: Solver Next) was used to observe the surface morphology of the films at a scanning range of 5.0 μm × 5.0 μm. The thickness of the film was characterized by spectroscopic ellipsometry (SE) on a WVASE32® apparatus from 240 to 1100 nm wavelength (5.16–1.12 eV) at an incidence angle of 65°. A combined Tauc-Lorentz oscillator model was selected to fit the obtained TiO_2 spectra. The transmission, reflectivity, absorbance and the self-cleaning of the as-deposited films were obtained on a UH4150 UV-Vis-NIR spectrophotometer. Meanwhile, Essential MacLeod software was used to simulate and analyse the optical properties of the film, which can provide theoretical support for the experiment. During the photocatalytic performance testing, a 200 W xenon lamp was used to simulate a solar light source (300–800 nm). The total irradiation time was 60, 120 and 180 min. The catalytic efficiency of the as-deposited film can be determined by the absorption peak strength of methyl orange solution at 460 nm obtained from UH4150 UV-Vis-NIR spectrophotometer.

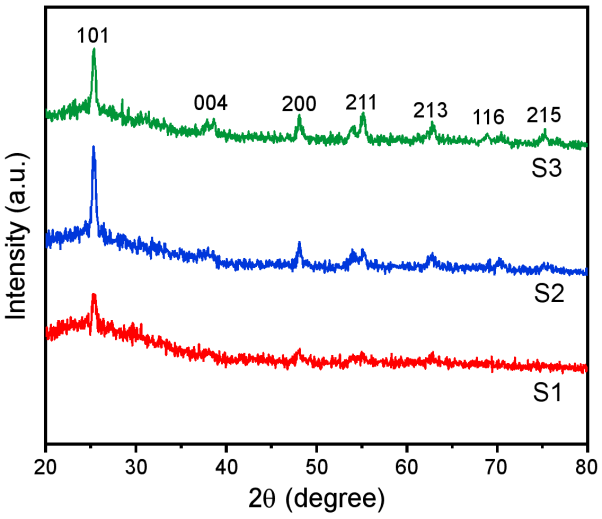

Figure 2. XRD patterns of TiO_2 films prepared for different sputtering times

III. Results and discussion

3.1. XRD analysis of TiO_2 films

The phase analysis of the samples was carried out by X-ray diffraction (XRD) and XRD patterns of TiO_2 films prepared for different sputtering times are shown in Fig. 2. All the samples showed the characteristic peak of anatase phase of TiO_2 and no rutile phase was observed. This is because the anatase phase is the result of the reaction between neutral Ti and neutral O_2 or O^-, while the rutile phase is formed by the reaction between Ti^+ and $O_2{}^+$, and the energy distribution intensity of positive ions in the sputtering plasma is heavily dependent on the total pressure [15]. Similarly, it is reported that under high sputtering pressure, whatever $O_2{}^+$ ions exist in the sputtering cavity may have very small energy, which may be the reason why there is no rutile phase in the sample [16]. In this experiment, the sputtering power and pressure are both large, and the prepared TiO_2 films show the characteristic peak of anatase phase. As it can be seen from Fig. 2, the crystallinity of the sample S1 prepared with a short sputtering time is not well-defined and the crystallinity of the film increases with the increase of sputtering time. The sample S3 has higher peak intensity and well-defined anatase characteristic peaks, including (101), (004), (200), (211), (213), (116), (215) (PDF 73-1764), but the sample S2 has the strongest (101) characteristic peak, forming anatase type TiO_2 film with (101) crystal face selective growth.

3.2. Thickness of TiO_2 films

According to different measurement forms, spectroscopic ellipsometry (SE) can be divided into reflection ellipsometry, transmission ellipsometry and scattering ellipsometry. Reflection ellipsometry is widely used as an important tool for the analysis of film thickness and optical properties. Its basic principle is shown in Fig. 3.

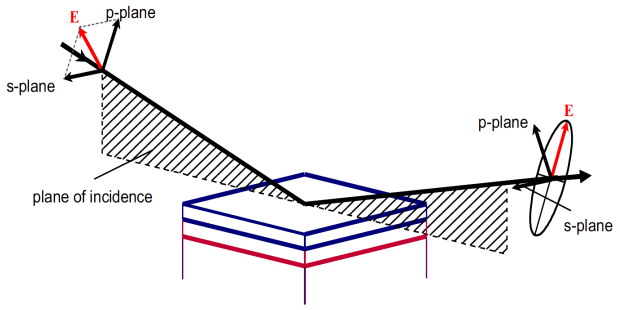

Figure 3. Schematic diagram of the sample measured by the reflective ellipsometry

The film thickness of the TiO_2 films can be measured by SE [17–19]. Firstly, elliptic partial parameters ψ and Δ can be obtained by SE and then the films' thickness and optical parameters are analysed by building a general oscillator model to fit SE data. Parameters ψ and Δ can be defined as [20]:

$$\rho(N^*, d) = \frac{\widetilde{R_p}}{\widetilde{R_s}} = \tan\psi \cdot \exp(i\Delta) \tag{1}$$

where $\widetilde{R_p}$ and $\widetilde{R_s}$ are the complex reflection coefficients of parallelly and perpendicularly polarized light parallel and perpendicular to the incident plane, respectively, N^* is the complex refractive index of the film and d is the film thickness.

The universal oscillator model was used to describe the TiO_2 film during fitting [21]. According to this model (composed of the Tauc-Lorentz oscillator model [22]), the ellipsoidal data of the measured TiO_2 film was fitted. According to the Tauc-Lorentz oscillator model, the complex dielectric constant of the TiO_2 film can be expressed as [21]:

$$\varepsilon = \varepsilon_1 + i\varepsilon_2 = \sum_{n=1}^{3} \varepsilon_n \tag{2}$$

$$\varepsilon_n = \varepsilon_{n1} + i\varepsilon_{n2} \tag{3}$$

$$\varepsilon_{n2} = \frac{A_n \cdot E_{0n} \cdot C_n \cdot (E - E_{gn})^2}{(E^2 - E_{0n}^2)^2 + C_n^2 \cdot E^2} \cdot \frac{1}{E},\ E > E_{gn} \tag{4a}$$

$$\varepsilon_{n2} = 0,\ E \le E_{gn} \tag{4b}$$

$$\varepsilon_{n1} = \frac{2}{\pi} \cdot P \cdot \int_{E_{gn}}^{\infty} \frac{\xi \cdot \varepsilon_{n2}(\xi)}{\xi^2 - E^2}\, \mathrm{d}\xi \tag{5}$$

where, P is the main part of the Cauchy integral, A_n and C_n are constants, E_{0n} is the central position of the oscillator and E_{gn} is the central vibration energy of the oscillator.

The thickness of the film was measured by SE method on a WVASE32® apparatus and fitted by the software of the instrument itself. The mean square error (MSE) was used to estimate the matching quality

between the data calculated by the model and the experimental data. The smaller the MSE value is, the higher the fitting accuracy is.

Figure 4 shows the fitting results of the sample S2 with an incident angle of 65° under the Tauc-Lorentz model. The solid line is the experimental result and the dashed line is the fitting result, the overall thickness of the film obtained by fitting was about 42 nm. Table 2 gives the thickness and surface roughness obtained by fitting the SE data and MSE of the fits for the TiO_2 films deposited at different sputtering time. We can see that all the values of MSE are below 5, which means the fitted results are credible. As shown in Fig. 5, it can be

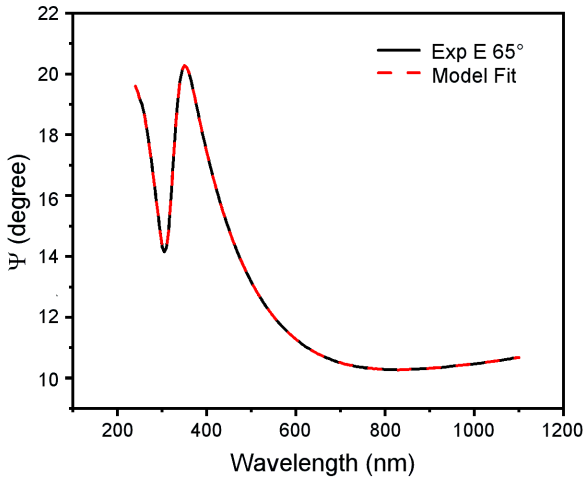

Figure 4. Experimental and fitted curves obtained by SE of sample S2

Table 2. Thickness, surface roughness and MSE of samples S1, S2 and S3 obtained from SE data

Sample	Thickness [nm]	Roughness [nm]	MSE [%]
S1	24.5	0	1.37
S2	42.4	0.1	0.73
S3	56.0	6.4	4.63

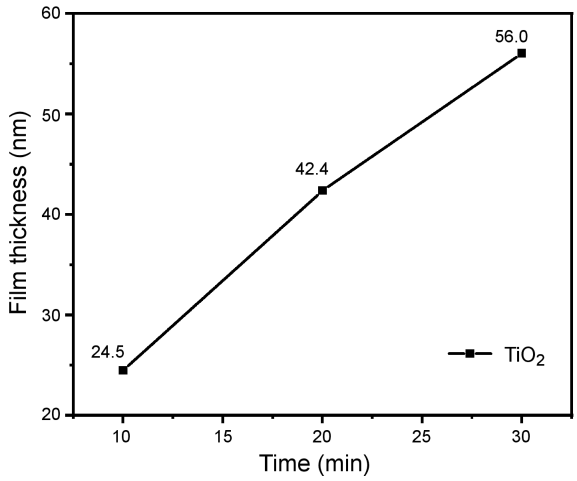

Figure 5. Thickness of TiO_2 films at different sputtering times

seen that the thickness of the films increases with the increase of sputtering time. The average deposition rate of the TiO_2 films under this condition was calculated to be 2.13 nm/min.

3.3. Optical properties of TiO_2 films

Essential MacLeod is an optical thin film calculation and analysis software, which is based on the basic theory and calculation of optical thin film. It can run under Microsoft Windows operating system and has a true multi-document interface, which is the most complete thin film computing and analysis software on the market today. It provides a complete set of performance calculation functions, which can calculate the characteristic parameters of a given optical film, not only the reflectivity, transmittance and phase, but it also can calculate the parameters including density, absorption rate, colour, overspeed, the amount of elliptic polarization and light dispersion, as well as the 0-3 derivative of wavelength [23]. Therefore, Essential MacLeod software can be used to simulate the optical properties of the film, providing theoretical support for the experiment.

Figures 6a and 6c show the transmission and reflection spectra of the samples S1, S2 and S3. As it can be seen, all the samples in the visible and near-infrared range showed high transmittance (between 60–95%) and low reflectivity (between 5–35%). The transmittance increased with the increase of wavelength and reflectance decreased with the increase of the wavelength. When the sputtering time is increased from 10 to 30 min, the transmittance decreases in the visible and near-infrared light range, meanwhile the reflectance increases. The transmittance at the wavelength of 550 nm band, the most sensitive to human eyes, decreases from 72.5% to 70.5%. Figures 6b and 6d show the transmission spectrum and reflection spectrum of the samples S1, S2 and S3 simulated by the Essential MacLeod software based on the film thickness from SE. In the range of visible and near-infrared light, the matching degree with the measured data (Figs. 6a and 6c) is high and maintains the same trend, which verifies the accuracy of the experimental results. With the increase of sputtering time, the wave peaks in the transmitted and reflected spectra move to the long wave direction and appear as "red shift". This may be due to the increase of sputtering time. The number of sputtering atoms reaching the substrate increases, which enables them to carry out effective migration and diffusion on the substrate. According to the SE results, the thickness of the film is increased. From the perspective of film crystallinity in the XRD pattern, the film crystallinity is more complete, resulting in the "red shift" of the wave peak in the transmission spectrum.

3.4. Optical band gap energies of TiO_2 films

Figure 7 shows the optical absorbance of the obtained TiO_2 films in the wavelength range of 300–1500 nm. It is obvious that all the samples showed high absorbance

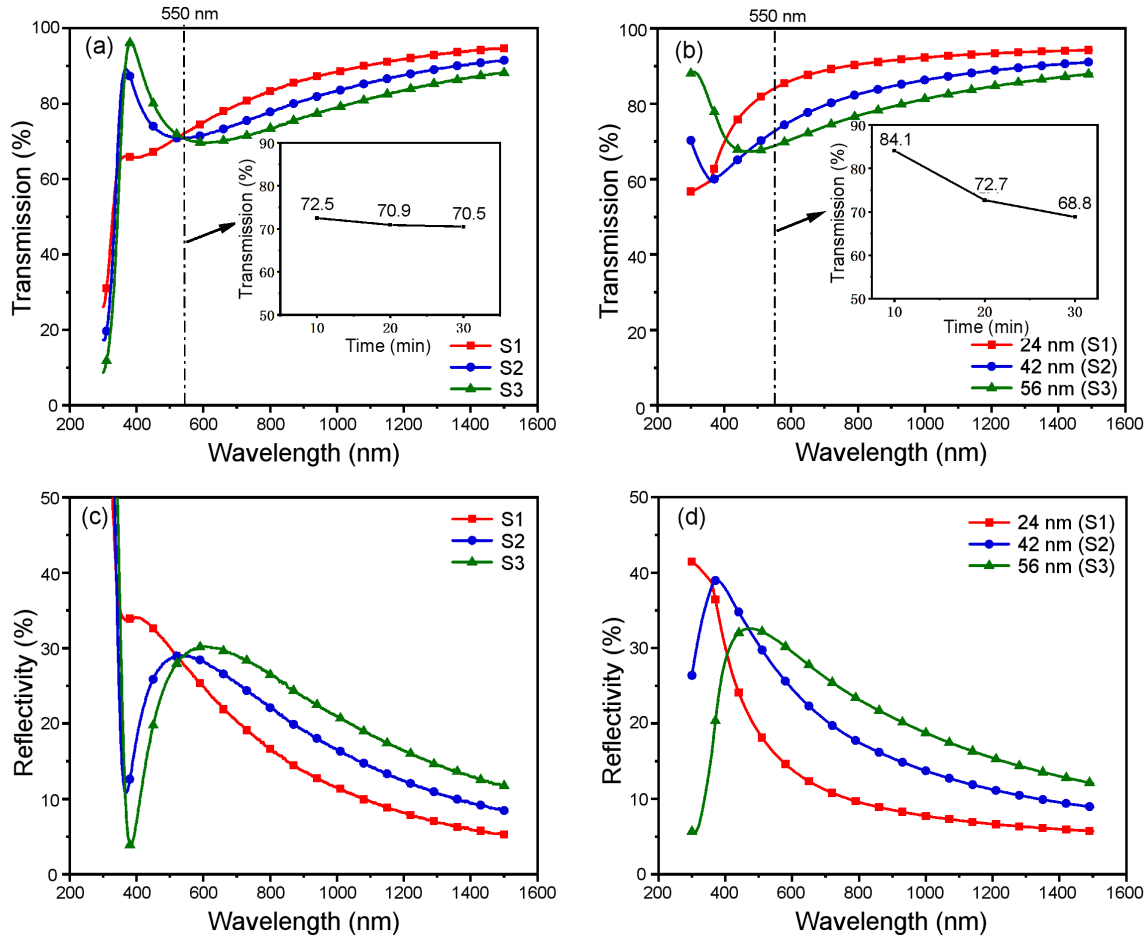

Figure 6. Transmission and reflection spectra of samples S1, S2 and S3 measured by UH4150 UV-Vis-NIR spectrophotometer (a and c) and simulated by Essential MacLeod software (b and d)

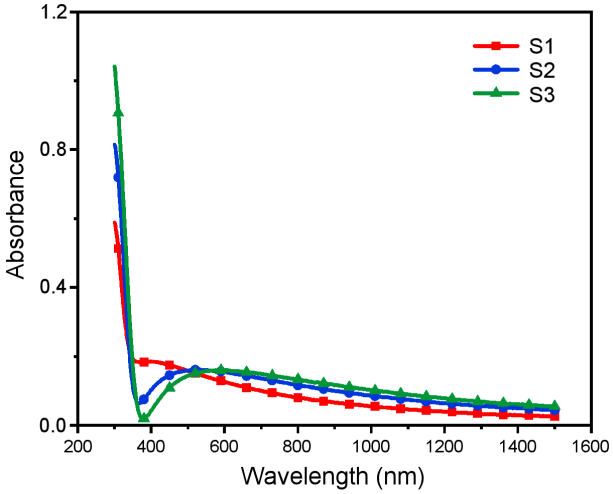

Figure 7. Optical absorbance of TiO_2 films sputtered for different sputtering times

in the wavelength range of 300–350 nm. The light absorbance increases with the increase of sputtering time, showing a strong light absorbance, and decreases sharply with the increase of wavelength. In the visible region, the absorbance is very low and nearly close to 0. The decrease of absorbance means the weaker light absorption capacity, indicating the higher transmittance in the visible region. From Fig. 6a it can be seen that the transmittance rises sharply in the wavelength range of 300–350 nm and has a high transmittance in the visible range.

TiO_2 is a wide band gap semiconductor. The band gap width of the TiO_2 films can be determined by the experimental spectrum of optical absorbance according to the following formula [24]:

$$\alpha h\nu = A \cdot (h\nu - E_g)^m \tag{6}$$

where, α is the light absorption coefficient, $h\nu$ is the photon energy of the incident light, A is the edge width parameter and m is equal to ½ and 2 for direct and indirect transitions, respectively. The plots of $(\alpha h\nu)^2$ versus photon energy $h\nu$ for a direct bandgap transitions are represented in Fig. 8 for different deposition time.

The band gap of the TiO_2 films was determined by extrapolation. With the increase of sputtering time, the band gap of the TiO_2 films decreases from 3.67 to 3.55 eV. This is due to the increase of the light absorption coefficient caused by the increase of the film thickness with the increase of the sputtering time. It is reported that the change of the band gap width of the film was also related to the atomic spacing. The film surface

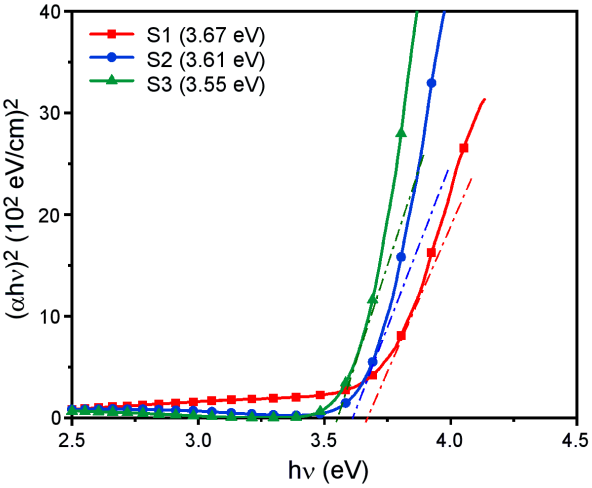

Figure 8. The curves of $(\alpha h\nu)^2$ versus photon energy $h\nu$ of samples S1, S2 and S3

mobility, the degree of crystal coalescence and the crystallinity of the sample all increase with the increase of sputtering time. This is consistent with the above XRD results. The higher crystallinity of the film may lead to the smaller atomic spacing, which is beneficial to decrease the band gap [24] of the obtained TiO_2 films.

3.5. AFM analysis of TiN/Ag/Cu_2O/TiO_2 films

AFM morphology of the TiN/Ag/Cu_2O/TiO_2 multilayer films is shown in Fig. 9. It can be seen that the surface of the prepared TiN/Ag/Cu_2O/TiO_2 multilayer film is composed of some tiny particles, whose particle sizes are all in the nanometer scale. With the increase of the sputtering time of the outermost TiO_2 film, the surface grains of the multilayer film become smaller and the film grows more compactly.

The surface roughness (R_a) and root mean square roughness (RMS) of the TiN/Ag/Cu_2O/TiO_2 multilayer films are given in Fig. 10. As it can be seen, the surface roughness and root mean square roughness first increase and then decrease with the increase of sputtering time. It is clear that R_a and RMS of the sample CF2 are the largest. Its specific surface area may be relatively large [25], which increases the contact area with methyl orange solution in the photocatalytic experiment, and thus CF2 may have stronger photocatalytic ability.

3.6. Optical properties of TiN/Ag/Cu_2O/TiO_2 films

It was confirmed that with the increase of sputtering time, the band gap of the TiO_2 thin films decreases (Fig. 7). However, the film thickness may also become higher, which may greatly influence the optical properties of the TiO_2 films. In order to decrease the band gap of the TiO_2 films, Cu_2O layer was introduced to prepare the multilayer films. It is reported that the theoretical band gap

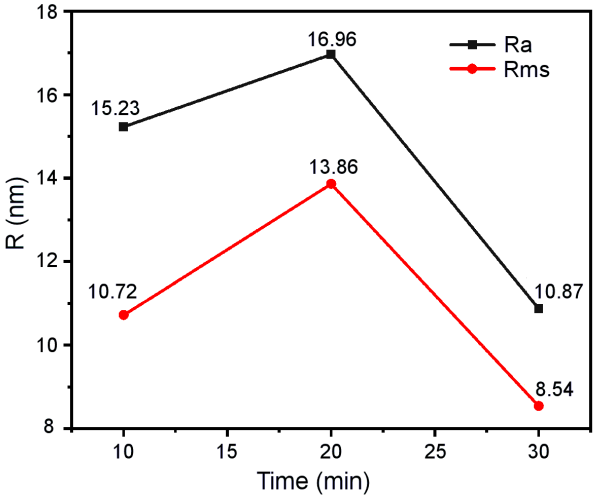

Figure 10. Surface roughness (R_a) and root mean square roughness (RMS) of TiN/Ag/Cu_2O/TiO_2 multilayer films

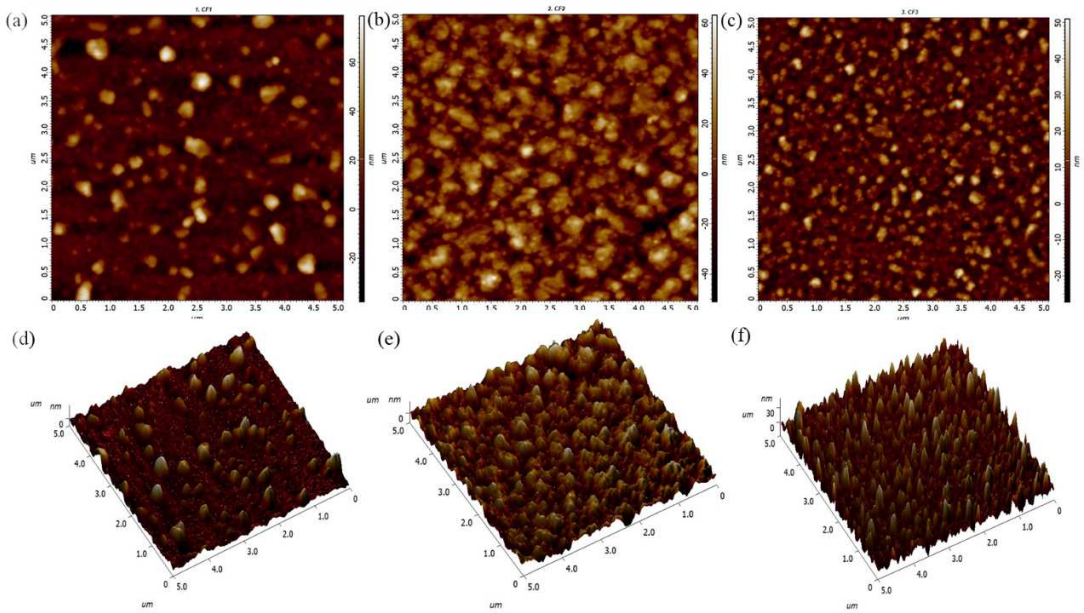

Figure 9. AFM morphology of TiN/Ag/Cu_2O/TiO_2: CF1 (a and d), CF2 (b and e) and CF3 (c and f) multilayer films

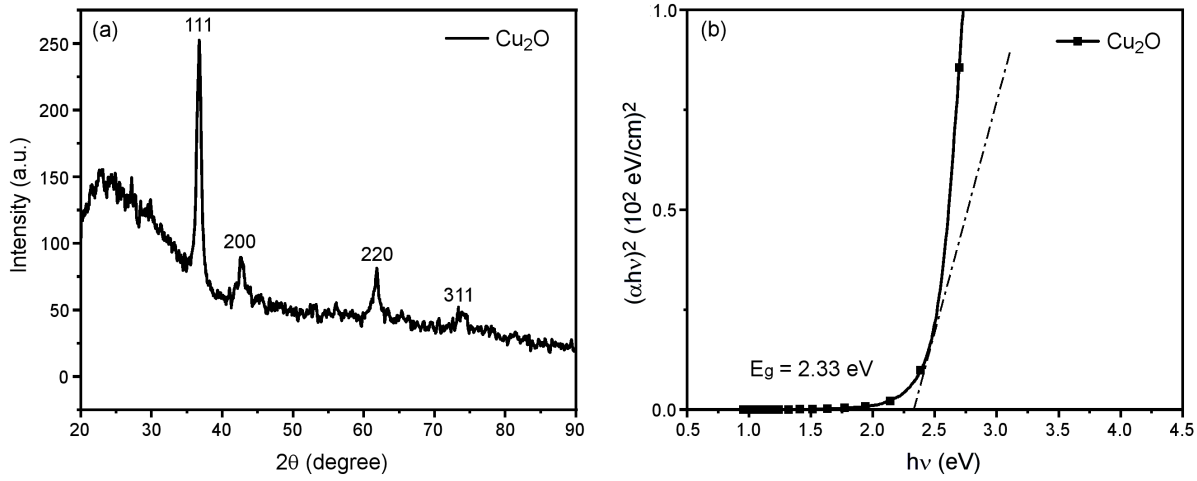

Figure 11. XRD pattern (a) and the relationship between $(\alpha h\nu)^2$ and $h\nu$ (b) of the Cu_2O film

of Cu_2O is $E_g \approx 2$–2.2 eV at pH = 7 [11] and can be combined with TiO_2 layer to form a p-n heterojunction. Figure 11a shows XRD pattern of Cu_2O film prepared under the deposition conditions given in Table 1. From Fig. 11b, we can see that the band gap of this Cu_2O film is 2.33 eV, which is close to the theoretical value.

Figure 12 shows optical properties of the obtained TiN/Ag/Cu_2O/TiO_2 multilayer films with different sputtering times of TiO_2 layer. The transmittance of the multilayer films in the visible region (380–780 nm) increases at first and then decreases with the increase of sputtering time. The transmittances of the multilayer films at the wavelength of about 550 nm are 55.6%, 66.6% and 34.5% for the CF1, CF2 and CF3, respectively (insert in Fig. 12a). According to Eq. 6, the band gap width of the multilayer film can be determined

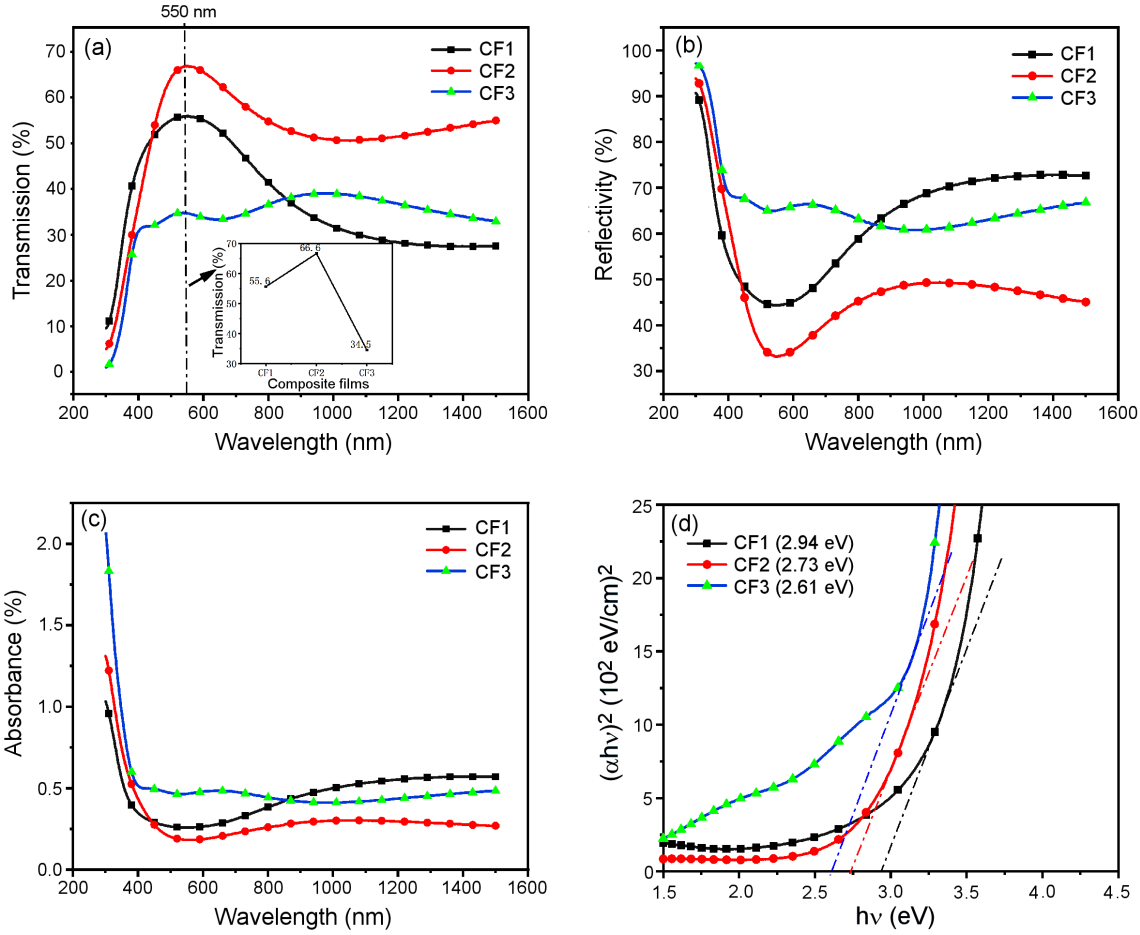

Figure 12. Optical properties of TiN/Ag/Cu_2O/TiO_2 multilayer films: transmission spectrum (a), reflection spectrum (b), absorption spectrum (c) and band gap width (d) of CF1, CF2 and CF3 films

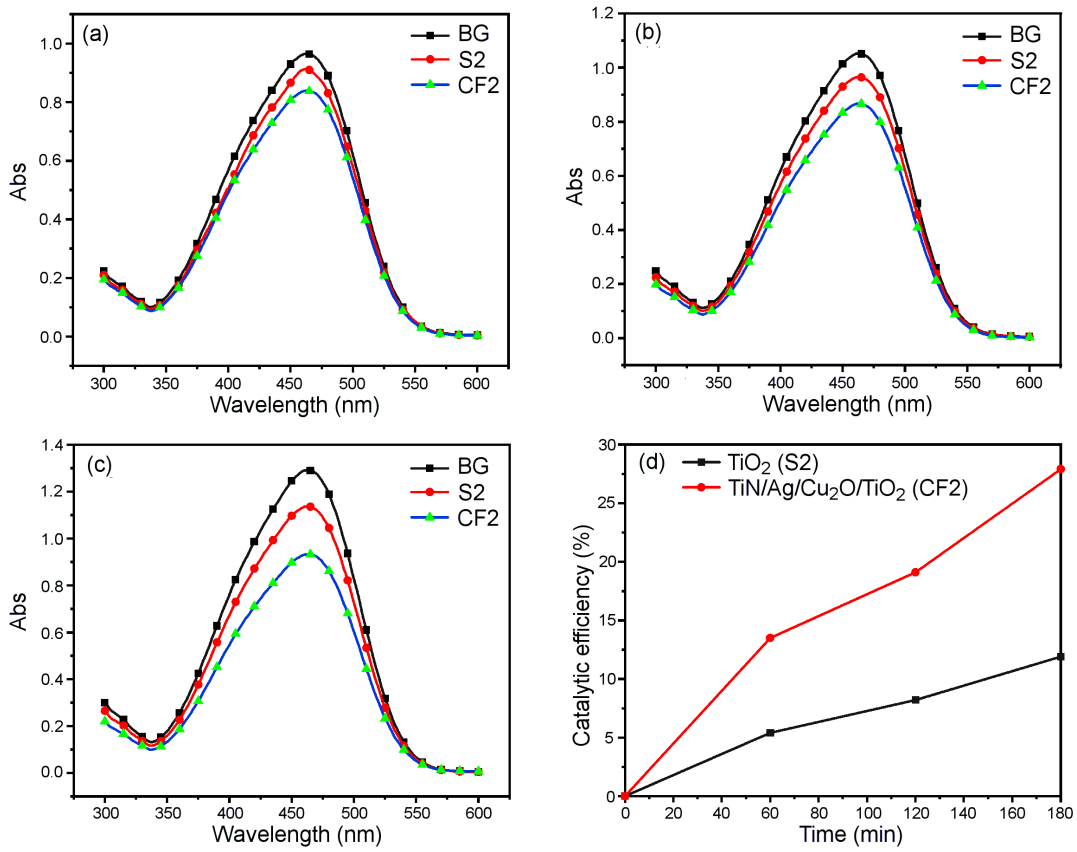

Figure 13. Absorption spectra of the sample in methyl orange solution at different times: a) 60 min, b) 120 min and c) 180 min. Catalytic efficiency of the films for methyl orange degradation (d)

by extrapolation from the absorption spectrum in Fig. 12c. As shown in Fig. 12d, the band gaps width of the CF1, CF2 and CF3 multilayer films are 2.94, 2.73 and 2.61 eV, respectively. Compared with those of the TiO_2 films (Fig. 8), the band gap widths of all multilayer films are significantly decreased. It is reported that n-type semiconductor TiO_2 with a larger band gap could be combined with p-type Cu_2O with a smaller band gap to form a p-n junction, thus reducing the TiO_2 band gap width and helping to improve the photocatalytic efficiency [9]. On the other hand, the optimal TiN thickness was beneficial to improve the surface morphology and crystal structure of the films and at the same time could reduce the energy band gap of the films [26].

3.7. Photocatalytic behaviour of TiN/Ag/Cu₂O/TiO₂ films

Photocatalytic performance of the as-prepared films was obtained by testing the degradation rate of the methyl orange solution. The faster the degradation rate of the methyl orange solution is, the better the photocatalytic performance of the film is. That is to say, the faster degradation rate of the methyl orange solution means the film owns better catalytic efficiency (η), which can be calculated by the following formula [27]:

$$\eta = \frac{C_0 - C_t}{C_0} \times 100 = \frac{A_0 - A_t}{A_0} \times 100 \qquad (7)$$

where, C_0 is the concentration of methyl orange solution before photocatalytic degradation, C_t is the concentration of methyl orange solution after photocatalytic degradation for time t; A_0 is the absorbance of methyl orange solution before photocatalytic degradation, A_t is the absorbance of methyl orange solution after photocatalytic degradation for time t. The catalytic efficiency of the as-deposited film can be determined by measuring the absorption peak strength of methyl orange solution at the wavelength of 460 nm obtained from UH4150 UV-Vis-NIR spectrophotometer.

Figure 13 shows the absorption spectra of the samples in methyl orange solution at different times, where BG represents the blank glass without film on the substrate. The catalytic efficiency of the thin film for methyl orange solution was calculated by Eq. 7 and shown in Fig. 13d. With the extension of the illumination time, the catalytic efficiency of the film has been increased. Compared with the TiO_2 films, the catalytic efficiency of the $TiN/Ag/Cu_2O/TiO_2$ multilayer films increased from 11.9% to 27.8% after 180 min irradiation, and the catalytic efficiency was significantly improved.

It is reported that Cu_2O-TiO_2 has a narrower band gap, which expands the optical absorption range of the material to 800 nm [10]. From the above analysis, one can easily see that the catalytic efficiency of the sample CF2 is higher than that of the sample S2. This may be due to the formation of p-n heterojunction between

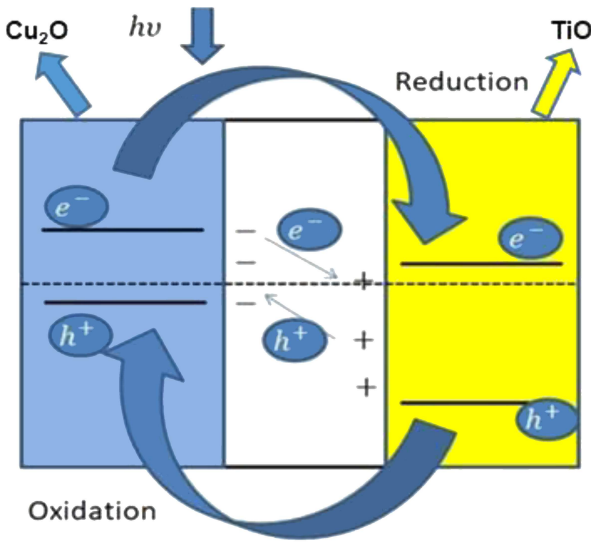

Figure 14. Photocatalytic mechanism of p-n Cu_2O-TiO_2 heterojunction system

TiO_2 and Cu_2O in the CF2. Figure 14 shows the photocatalytic mechanism of the Cu_2O-TiO_2 p-n type heterojunction system. According to the calculated values above, the band gaps of the as-prepared TiO_2 and Cu_2O films are about 3.61 and 2.33 eV, respectively. The conduction band and valence band of Cu_2O are higher than those of TiO_2. When the incident light energy is higher, inter-band intrinsic excitation transition will occur between valence band electrons both in TiO_2 and Cu_2O. Due to the energy level difference between conduction band and valence band of different semiconductors, photogenerated electrons will transit from the conduction band of Cu_2O to the conduction band of TiO_2 in our case, resulting in the accumulation of the electrons in TiO_2 and the holes in Cu_2O. Hence, the separation of photoproduced electrons and holes is promoted and the recombination probability of photogenerated electron-hole pairs is reduced. On the other hand, when the incident light energy is weak, only Cu_2O can undergo inter-band transition and the excited electrons will also be transferred to the TiO_2 conduction band. The photogenerated carriers can be separated effectively and the carrier life can be extended, which leads to the improvement of the photocatalytic efficiency. At the same time, the outermost TiO_2 film has stable chemical properties, corrosion resistance and wear resistance, which can prevent Cu_2O film from direct contact with the air, thus reducing the possibility of Cu_2O being oxidized by oxygen in the air. This also can increase the life of the photocatalytic film. As for the effect of Ag film, it is reported that when Cu_2O contacts directly with Ag nanoparticles, the effective hole consumption of the valence band can be found. The formation of the interface between Cu_2O and Ag particles not only did enhance the photostability of Cu_2O, but also it inhibited the photo-corrosion and oxidation of Ag to Ag^+, which may improve the overall photocatalytic performance significantly [5].

From Fig. 12d, the band gap width of the CF2 is 2.73 eV, corresponding to the wavelength of about 454 nm. This indicates that the spectral response range of the multilayer film is expanded to the visible region. Compared with the spectral response range of the TiO_2 (only in ultraviolet light region), the photocatalytic efficiency of the multilayer films was improved and the utilization of sunlight was expanded. It is worth to mention that in Fig. 12b, the lowest reflectivity of the multilayer films in near infrared region is about 50%, indicating that the multilayer film also possesses the performance of low emission (Low-e) films. That is to say, the TiN/Ag/Cu_2O/TiO_2 multilayer films we designed not only photocatalytic activity, but also Low-e performance. More detailed research of this kind of multilayer film will be carried out in the future.

IV. Conclusions

TiO_2 thin films were prepared on glass substrates by DC-RF multifunctional magnetron sputtering apparatus. The effects of sputtering time on the crystal structure and optical properties of the thin films were studied. The results show that the prepared TiO_2 films are all anatase type. The band gap of the as-prepared TiO_2 film is relatively high and its spectral response range is restricted in the ultraviolet region. Based on the studies of the TiO_2 thin films, TiN/Ag/Cu_2O/TiO_2 multilayer films were designed and prepared successfully. In the multilayer films p-n heterojunction is formed between Cu_2O and TiO_2 and the band gap of TiO_2 film can be reduced significantly. This expands the spectral response range of the TiO_2 film from ultraviolet light region to visible light region. The photocatalytic efficiency of the multilayer film was also improved compared with that of the single TiO_2 film. In conclusion, there is a prospect to improve optical properties of TiO_2 film by optimal design of multilayer films.

Acknowledgements: This work was supported by the National Science Foundation of China (No. 11574276, 11874328), key science and technology research projects of Henan Province (No.192102310299), the Foundation and frontier technology research project of Henan Province (No. 152300410038) and the Natural Science Foundation of Henan Province (No. 182300410192).

References

1. A. Fujishima, K. Honda, "Electrochemical photolysis of water at a semiconductor electrode", *Nature*, **238** (1972) 37–38.
2. J.C. Lim, K.J. Song, C. Park, "The effect of deposition parameters on the phase of TiO_2 films grown by RF magnetron sputtering", *J. Korean Phys. Soc.*, **65** (2014) 1896–1902.
3. F. Chaabouni, L.C. Costa, , M. Selmi, M. Abaad, B. Rezig, "Influence of deposition time on properties of the RF sputtered TiO_2 thin films", *Mater. Sci. Forum*, **587-588** (2008) 824–828.

4. M.C. Liao, H. Niu, G.S. Chen, "Effect of sputtering pressure and post-annealing on hydrophilicity of TiO_2 thin films deposited by reactive magnetron sputtering", *Thin Solid Films*, **518** (2010) 7258–7262.
5. M. Okada, M. Tazawa, P. Jin, Y. Yamada, K. Yoshimura, "Fabrication of photocatalytic heat-mirror with TiO_2/TiN/TiO_2 stacked layers", *Vacuum*, **80** (2006) 732–735.
6. C.Y. Toe, J.S.R. Amal, Y.H. Ng, "Recent advances in suppressing the photocorrosion of cuprous oxide for photocatalytic and photoelectrochemical energy conversion", *J. Photochem. Photobio. C Photochem. Rev.*, **40** (2019) 191–211.
7. Y. Xiao, H. Zhang, "Tunable optical properties of SiO_2/Ag double-layer and SiO_2/Ag/SiO_2 triple-layer hybrid structures", *Phys. B Condensed Matter*, **605** (2021) 412772.
8. H. Wang, C. Tang, Q. Shi, M. Wei, Y. Su, S. Lin, M. Dai, "Influence of Ag incorporation on the structural, optical and electrical properties of ITO/Ag/ITO multilayers for inorganic all-solid-state electrochromic devices", *Ceram. Int.*, **47** [6] (2020) 7666–7673.
9. H. Zhu, Y. Li, X. Jiang, "Room-temperature synthesis of cuprous oxide and its heterogeneous nanostructures for photocatalytic applications", *J. Alloys Compd.*, **772** (2019) 447–459.
10. L. Yan, F. Yang, C.Y. Tao, X. Luo, "Highly efficient and stable Cu_2O-TiO_2 intermediate photocatalytic water splitting", *Ceram. Int.*, **46** [7] (2020) 9455–9463.
11. M.E. Aguirre, R. Zhou, A.J. Eugene, M.I. Guzman, M.A. Grela, "Cu_2O/TiO_2 heterostructures for CO_2 reduction through a direct Z-scheme: Protecting Cu_2O from photocorrosion", *Appl. Cataly. B Environm.*, **217** (2017) 485–493.
12. Z. Hu, X. Wang, H. Dong, S. Li, X. Li, L. Li, "Efficient photocatalytic degradation of tetrabromodiphenyl ethers and simultaneous hydrogen production by TiO_2-Cu_2O composite films in N_2 atmosphere: Influencing factors, kinetics and mechanism", *J. Hazard. Mater.*, **340** (2017) 1–15
13. Q. Ding, S. Chen, D. Chen, J. Liang, C. Liu, "Preparation and photocatalytic property of Cu_2O-TiO_2 composite nanotube arrays film by the anodic oxidation", *Surf. Interfaces*, **4** (2016) 35–41.
14. J. Li, L. Liu, Y. Yu, Y. Tang, H. Li, F. Du, "Preparation of highly photocatalytic active nano-size TiO_2-Cu_2O particle composites with a novel electrochemical method", *Electrochem. Commun.*, **6** [9] (2004) 940–943.
15. K. Okimura, A. Shibata, N. Maeda, K. Tachibana, Y. Noguchi, K. Tsuchida, "Preparation of rutile TiO_2 films by RF magnetron sputtering", *Jpn. J. Appl. Phys.*, **34** [Part 1, 9A] (1995) 4950–4955.
16. N. Martin, A.M.E. Santo, R. Sanjinés, F. Lévy, "Energy distribution of ions bombarding TiO_2 thin films during sputter deposition", *Surf. Coat. Technol.*, **138** [1] (2001) 77–83.
17. Q. Ma, X. Shi, L. Bi, J. Li, Q. Zhou, B. Zhu, "Influence of the deposition temperature on the optical and electrical properties of TiN film by spectroscopic ellipsometry", *Superlattices Microstruct.*, **151** (2021) 106815.
18. J.M. Zhao, P. Yang, "A method for determining ultrathin DLC film thickness by spectroscopic ellipsometry", *Microsystem Technol.*, **18** [9-10] (2012) 1455–1461.
19. X. Fan, H. Liu, X. Zhang, "Identification of optimal ALD process conditions of Nd_2O_3 on Si by spectroscopic ellipsometry", *Appl. Phys. A*, **114** [2] (2013) 545–550.
20. H. Fujiwara, *Spectroscopic Ellipsometry: Principles and Applications*, John Wiley & Sons, 2007.
21. A. Biswas, D. Bhattacharyya, H.C. Barshilia, N. Selvakumar, K.S. Rajam, "Spectroscopic ellipsometric characterization of TiAlN/TiAlON/Si_3N_4 tandem absorber for solar selective applications", *Appl. Surf. Sci.*, **254** [6] (2008) 1694–1699.
22. M.J. Devries, C. Trimble, T.E. Tiwald, D.W. Thompson, J.A. Woollam, "Optical constants of crystalline WO_3 deposited by magnetron sputtering", *J. Vacuum Sci. Technol. A*, **17** (1999) 2906–2910.
23. O.K. Simya, K. Balachander, D. Dhanalakshmi, A.M. Ashok "Performance of different anti-reflection coating and TCO layers for kesterite based thin film photovoltaic devices using Essential Macleod simulation program", *Superlattice Microstruct.*, **145** (2020) 106579.
24. M.F. Hossain, P. Paul, T.Takahashi, "Effect of deposition time on structural, optical and morphological properties of facing-target sputtered TiO_2 thin film", pp. 241–244 in *2015 International Conference on Electrical & Electronic Engineering (ICEEE)*. IEEE, 2015.
25. R. Chopra, F. Podczeck, G. Alderborn, "The influence of film coating on the surface roughness and specific surface area of pellets", *Part. Part. Syst. Char.*, **19** (2002) 277–283.
26. M.A. Awad, A.H., Aly "Experimental and theoretical studies of hybrid multifunctional TiO_2/TiN/TiO_2", *Ceram. Int.*, **45** [15] (2019) 19036–19043.
27. C. Shifu, C. Gengyu, "Photocatalytic degradation of organophosphorus pesticides using floating photocatalyst $TiO_2 \cdot SiO_2$/beads by sunlight", *Solar Energy*, **79** [1] (2005) 1–9.